

Detecting Hybrid and Electric Vehicles Using a Smartphone

ABSTRACT

Pedestrians have difficulty noticing hybrid vehicles (HVs) and electrical vehicles (EVs) quietly approaching from behind. We propose a vehicle detection scheme using a smartphone carried by a pedestrian. A notification of a vehicle approaching can be delivered to wearable devices such as Google Glass. We exploit the high-frequency switching noise generated by the motor unit in HVs and EVs. Although people are less sensitive to these high-frequency ranges, these sounds are prominent even on a busy street, and it is possible for a smartphone to detect these signals. The ambient sound captured at 48 kHz is converted to a feature vector in the frequency domain. A J48 classifier implemented on a smartphone can determine whether an EV or HV is approaching. We have collected a large amount of vehicle data at various locations. The false-positive and false-negative rates of our detection scheme are 1.2% and 4.95%, respectively. The first alarm was detected as early as 11.6 s before the vehicle approached the observer. The scheme can also determine the vehicle speed and vehicle type.

Author Keywords

Hybrid Vehicles; Electric Vehicles; Smartphone Sensing

ACM Classification Keywords

H.3.4. Systems and Software

INTRODUCTION

Hybrid vehicles (HVs) and electric vehicles (EVs) are becoming more reasonable choices for consumers. According to a sales report in Japan, HVs comprise 29.7% of all new cars sold in 2012[6]. Even though the retail price of HVs and EVs tends to still be higher than that of gasoline- and diesel-engine vehicles, the fuel consumption and the quietness of HVs and EVs, especially in the lower speed range of approximately 0-30km/h, is significantly better[3](Figure 1). However, this quietness has caused a new social problem. In [9], it is reported that a robber approached a pedestrian from behind using an HV and snatched the handbag of the victim. The quietness of the vehicle makes it more difficult for pedestrians to notice HVs and EVs approaching from behind. According to the NHTSA[7], HVs cause twice as many vehicle-to-pedestrian accidents as combustion engine cars when reversing or parking at slow speeds. Similarly, an increase in EV/HV-to-bicycle accidents has also been reported. As the

numbers of EVs and HVs are increasing, there is a general need to solve this problem.

To cope with this problem, some EV and HV models are equipped with external speakers that generate artificial “electric vehicle warning sounds,” which allow pedestrians to be alerted to the approach of the vehicle. Although the sound is sufficiently quiet for drivers in the car, this solution is not considered smart because it loses the benefit of the quietness of the vehicles. Additionally, some drivers switch off this warning sound. Vehicular communication systems have been proposed by many researchers[8][4]. Using a dedicated short-range communication (DSRC) system or cellular communication system, a vehicle or infrastructure transmits a wireless communication message to mobile terminals even when they are out of sight. This is a promising approach when such communication protocols are equipped in both of the cars and user terminals. However, it is preferable if a device carried by a user can detect the approach of vehicles without the explicit support of cars and infrastructure.

In this study, we exploit the high-frequency acoustic noise generated by EVs and HVs. It is not inaccurate to state that almost all modern HVs and EVs generate switching noise at approximately 5, 10, 15 and 20 kHz because of the internal mechanism of the electrical propulsion system. This switching noise contains considerable useful information such as the vehicle speed and vehicle type. Because the original switch-

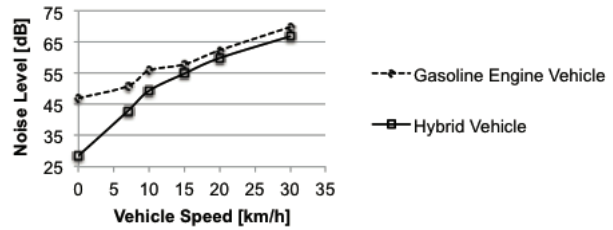


Figure 1. Differences in noise level between HVs and gasoline engine vehicles. HVs are quieter at speeds less than 30 km/h.

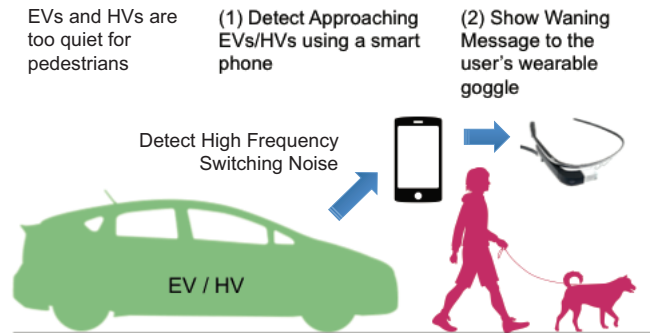


Figure 2. The concept of the proposed system. An approaching EV/HV is detected by the smartphone of a user. The user is notified of the message by a wearable display.

Permission to make digital or hard copies of all or part of this work for personal or classroom use is granted without fee provided that copies are not made or distributed for profit or commercial advantage and that copies bear this notice and the full citation on the first page. Copyrights for components of this work owned by others than ACM must be honored. Abstracting with credit is permitted. To copy otherwise, or re-publish, to post on servers or to redistribute to lists, requires prior specific permission and/or a fee. Request permissions from Permissions@acm.org.

Ubicomp '14, September 13 - 17 2014, Seattle, WA, USA
Copyright 2014 ACM 978-1-4503-2968-2/14/09...\$15.00.
<http://dx.doi.org/10.1145/2632048.2632088>

ing frequency is known, it is also possible to detect the relative speed between the vehicle and an observer (a pedestrian) on the basis of the Doppler shift of the noise.

Our experimental results show that these switching sounds are prominent in ambient noise both on a busy street and in a quiet residential area. Although people are relatively insensitive to these high frequencies, we found that the switching noise was easily detectable using a common handheld device such as a smartphone. The recognition mechanism is sufficiently simple to be performed on a smartphone.

The rest of this paper is organized as follows. In the next section, we show the recording results of the switching noise generated by EVs and HVs and discuss what type of information is available via the analysis of the switching noise. Then, we introduce our EV/HV detection scheme, followed by the evaluation results. Implementation on an Android smartphone and Google Glass is demonstrated. Related works are introduced before concluding this paper.

SWITCHING NOISE FROM EVS AND HVs

Mechanism of Motors in EVs and HVs

Motors that drive EVs and HVs must be compact and energy efficient. For this reason, most EVs and HVs are equipped with an interior permanent magnet (IPM) synchronous motor. The speed of an IPM synchronous motor can be controlled by alternating the frequency of the input AC signal, typically using pulse-width modulation (PWM). PWM generates a sine-like wave using a series of short rectangular pulse waves. Semiconductor switches such as insulated-gate bipolar transistors (IGBTs) are used to generate short pulses for high conversion efficiency. Because of the properties of IGBTs, the switching speed of an IGBT is typically 5 or 10 kHz. This high-frequency current travels through the coil inside a motor, generating a mechanical sound. This acoustic noise is released into the air outside the vehicle. The rectangular wave in the noise also contains higher-order harmonics such as 15 and 20 kHz signals.

In order to analyze the switching noise from EVs and HVs, we have performed measurement experiments for different vehicles in three different environments, as shown in Figure 3. A Nissan Leaf (EV) and Toyota Prius PHV (HV) were chosen as target models. The measurements were performed in a quiet residential area, on a busy street and in a parking lot, where vehicle-to-pedestrian accidents are likely to happen. Each measurement was performed at speeds of 5, 10, 20, and 30 km/h. It is reported that HV/EVs and conventional vehicles are equally safe when traveling more than approximately 32 km/h, because the noise from the tires and wind generates most of the audible cues at those speeds[13].

EV warning sounds were turned off during the measurement. The observer held an iPod Touch (fourth generation) in hand and recorded ambient sound using a built-in microphone at a sampling rate of 48 kHz. The audio was saved in an uncompressed 16-bit monaural linear PCM audio format. During the recording, the mobile terminal was held by hand in front of the waist.



Figure 3. Snapshot of the environmental measurements.

The cars always approached from behind the observer and passed at a distance of 1.5 m. The measurements were repeated at each location at least five times for each speed, except on a busy street. On a busy street, the measurement was repeated three times at a speed of 30 km/h in order to avoid blocking traffic. The experiment was focused on a speed range less than 30 km/h because friction noise from the tires is dominant at speeds greater than 30 km/h.

The ambient noise levels were measured using a portable sound-level meter (Rion NA-28) and were 37.6 dB, 40.6 dB and 58.7 dB for the parking lot, residential area, and busy street respectively.

Measurement Results

Spectrograms of the captured ambient sound are shown in Figure 4 and 5. For the case of Nissan Leaf, switching noise was clearly detected at 10 and 20 kHz. On the other hand, the switching noise at 5 kHz is more prominent than that at 10 or 20 kHz for a Toyota Prius PHV.

The hearing range of normal people is from 20 Hz to 20 kHz, on average. However, it is claimed that there are large variations among individuals. Sensitivity to high frequencies declines with age. Thus, it is difficult for elderly pedestrians to notice high-frequency noises from EVs and HVs.

In each image in Figure 4, two or three S-shaped curves are observed. The reason the curves are S-shaped is because of the Doppler effect due to the movement of the car. According to the definition of the Doppler shift, the relationship between the observed frequency f and the emitted frequency f_0 is given by

$$f = \frac{c^2 f_0}{c^2 - v^2} \left\{ 1 - \frac{v^2 t}{\sqrt{c^2 v^2 t^2 + l^2 (c^2 - v^2)}} \right\} \quad (1)$$

where c is the velocity of sound, v is the velocity of the vehicle, l is the closest distance between the observer and the vehicle, and t is the time. The distance between the observer and the vehicle is shortest at $t = 0$.

On the basis of this relationship, we now calculate f_0 by fitting the data using the fitting function of gnuplot (Table 1).

f_{High} and f_{Low} in Table 1 represent f_0 of two independent S-shaped lines. The difference between the two frequencies ($f_{High} - f_{Low}$) increases with the speed of the vehicle. This is an important and unique feature of PWM motors. The speed

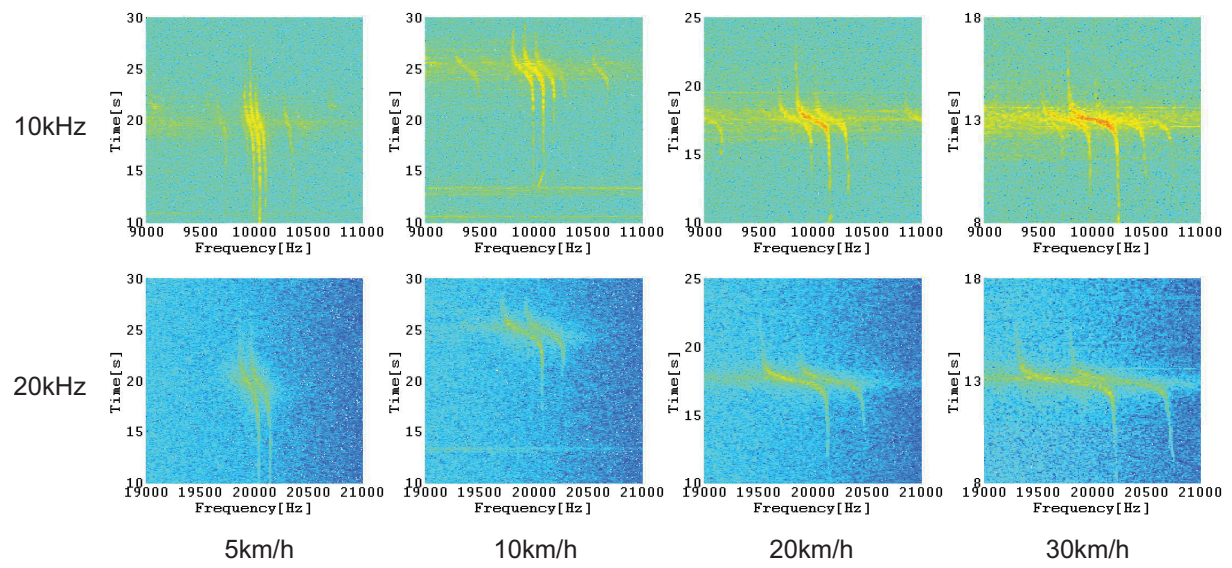


Figure 4. Spectrogram of an EV (Nissan Leaf). Switching noise is observed at 10 and 20 kHz.

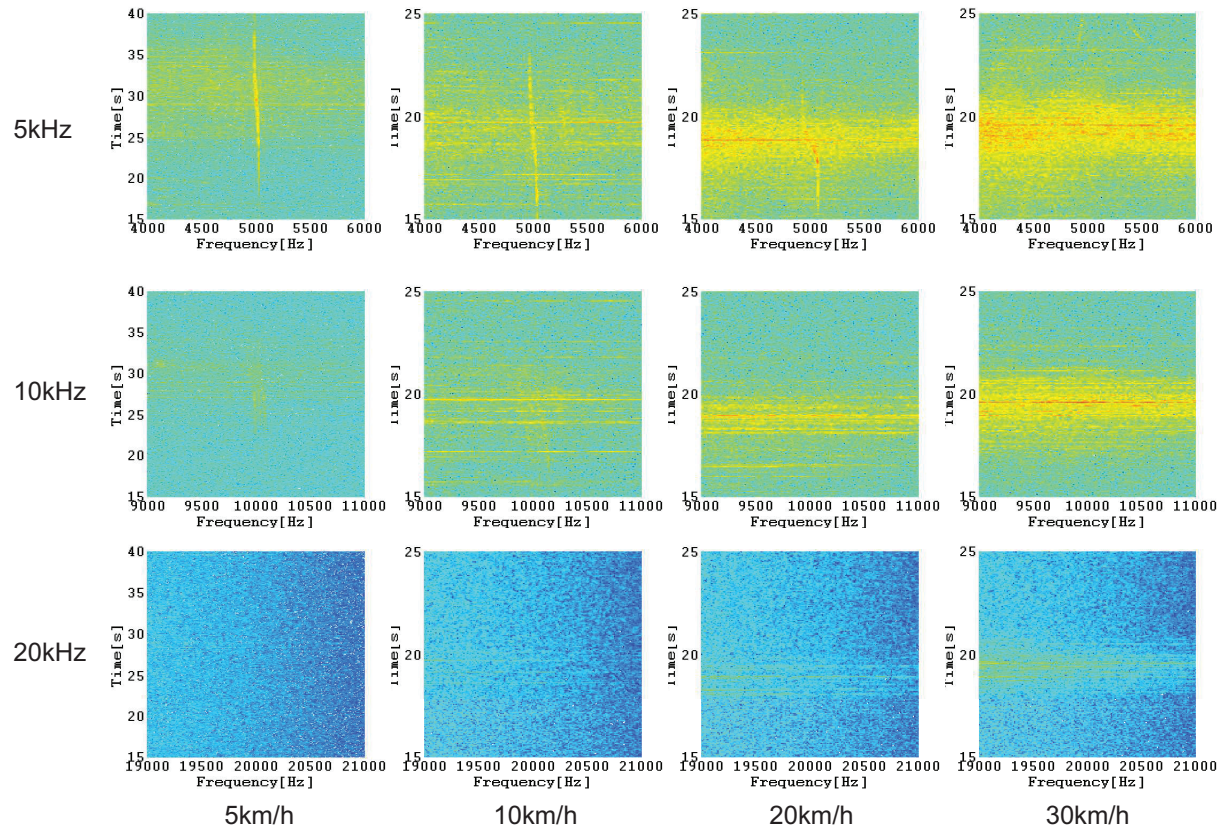
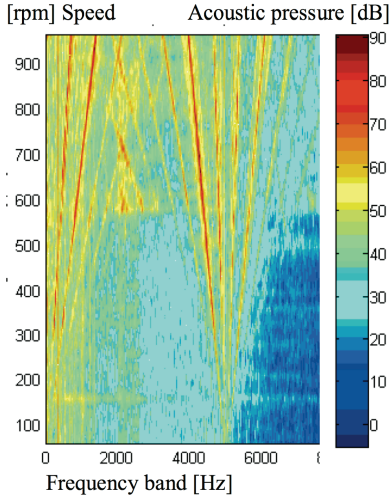


Figure 5. Spectrogram of an HV (Toyota Prius). Switching noise is observed at 5 kHz.

	10 km/h	20 km/h	30 km/h
f_{High}	2.010×10^4	2.018×10^4	2.023×10^4 Hz
f_{Low}	1.993×10^4	1.985×10^4	1.978×10^4 Hz
$f_{High} - f_{Low}$	170	330	450 Hz

Table 1. f_0 of EV at 20 kHz**Figure 6.** Acoustic pressure versus motor speed over the frequency band [2].

of an IPM synchronous motors is controlled by the modulation of the input power. The spectrum of the pulse waves is known to be split into multiple side bands[2] as shown in Figure 6. This is the reason that two or three S-shaped lines are observed in Figure 4 and implies that the observer can determine how fast the car is moving by only using audible information.

DETECTION SCHEME

In order to detect approaching EVs and HVs using a smartphone, the detection method must be simple and sufficiently fast enough for embedded devices. In addition, the detection scheme must be robust to variations in the ambient noise

level. However, the representation must not be too specific to a particular vehicle model and make. Moreover, the switching noise contains an abundance of useful information such as vehicle speed (due to the change in the modulation frequency) and direction from the perspective of the observer (due to the Doppler shift). Thus, the detection scheme should take advantage of such features.

In order to satisfy the above-mentioned requirements, we employ a machine learning approach. A flowchart of our detection scheme is shown in Figure 7.

Feature Vector

First, we create a “fingerprint” of each vehicle using the audio signal captured by a smartphone. We define a “frame” that consists of 32,768 raw audio samples (i.e. 0.683 s, sampling rate of 48 kHz). Each frame is then transformed into the frequency domain using fast Fourier transform (FFT). Then, some frequency segments in which typical switching noise appears are selected as summarized in Table 2. For each segment, the average and maximum values normalized by the total power for all frequencies are calculated. Normalization is necessary because of the sound-quality improvement technique named auto-gain control implemented in the smartphone. The combination of the average and maximum explains whether significant power exists in the specific frequency band. Thus, the feature vector has a total of 96 elements (3 frequency bands \times 16 segments \times 2 values).

Labeling

Each feature vector is then annotated with a label showing whether an approaching vehicle is present on the basis of the audible features. The label also contains information on the model and speed of the vehicle. The rest of the states (i.e., the vehicle is moving away, or no vehicles are present) are labeled as “no approaching vehicles” because outgoing vehicles do not harm pedestrians. To summarize, each feature vector is annotated with one of the following labels: No, ev5, ev10, ev20, ev30, hv5, hv10, hv20, and hv30. This labeling is manually performed offline. The label is then used to construct a decision tree that will be explained in the next section.

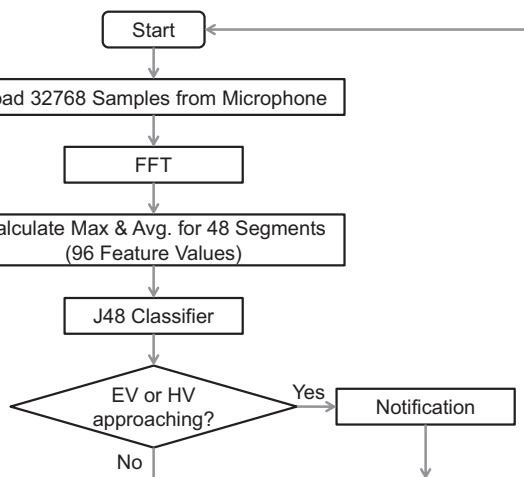
Supervised Learning

WEKA is a powerful and popular toolkit for data mining. We use a J48 decision tree as a classifier, which is a WEKA implementation of a C4.5 system.

The learning data were collected on a busy street, in a quiet residential area, and in a parking lot. Both the Nissan Leaf (EV) and Toyota Prius PHV (HV) were measured separately. The vehicles approached the observer at 5, 10, 20, and 30 km/h¹. The measurement was performed six times for each condition. The data set consists of a total of 1,552 labeled data points.

EVALUATION

First, we evaluate how the detection accuracy of EVs is affected by differences in ambient noise and vehicle speed. We

**Figure 7.** Flowchart of our detection scheme.

¹On a busy street, only data at 30 km/h are available.

Band	Beginning and end	Interval
5kHz	4600 Hz – 5400 Hz	50 Hz (16 segments)
10kHz	9200 Hz – 10800 Hz	100 Hz (16 segments)
20kHz	18400 Hz – 21600 Hz	200 Hz (16 segments)

Table 2. Segments

@Parking Lot		Recognition Result				
		no	ev5	ev10	ev20	ev30
Ground Truth	no	98.81%	0.00%	0.60%	0.30%	0.30%
	ev5(km/h)	2.99%	88.06%	7.46%	0.00%	1.49%
	ev10(km/h)	3.45%	8.62%	84.48%	3.45%	0.00%
	ev20(km/h)	0.00%	2.08%	4.17%	89.58%	4.17%
	ev30(km/h)	14.29%	0.00%	0.00%	4.08%	81.63%

Table 3. Confusion matrix of an EV moving at different speeds.

have performed 10-fold cross-validation for all the data captured in a parking lot (Par), in a residential area (Res), and on a busy street (Bus). There are 1,350 labeled data points used for this experiment is 1,350².

The results are listed in Table 3. The label “No” in the table represents a situation where no approaching EVs are detected, EVs moving away from the observer are also classified as “No” (as intended). From this table, a vehicle is misclassified in some cases as moving at the wrong speed. However, in terms of the application, this is not considered a severe misclassification unless the vehicle speed is crucial information. Now, we define the false-positive rate as the rate of instances when the classifier reported a vehicle (ev5, ev10, ev20, or ev30) when there was none and define the false-negative rate as the rate of instances when the classifier reported there were no approaching vehicles when the data are labeled as ev5, ev10, ev20, or ev30. The false-positive rate for all the data was 1.2% and the false-negative rate was 4.95%³.

Figure 8 shows the cumulative probability of the true-positive alarms detected until the vehicle passed by the observer. The figure shows that the approach of the EV was detected an average of 6.4 s before the vehicle passed by the observer.

²This number does not include the data for HVs.

³Note that this false negative rate was calculated on the basis of on all the data captured rather than a simple arithmetic calculation from Table 3.

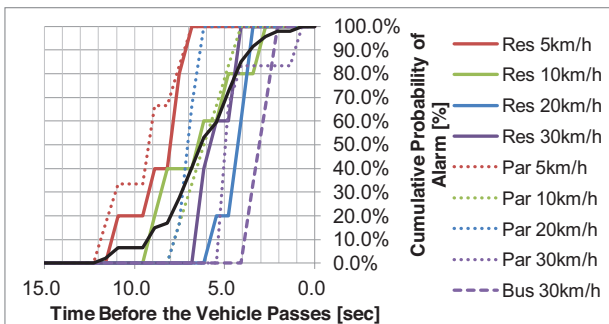


Figure 8. Cumulative probability of the alarms fired ahead of the arrival of the vehicle.

@Parking Lot		Recognition Result		
		no	ev	hv
Ground Truth	no	95.92%	0.35%	3.73%
	ev	6.31%	92.79%	0.90%
	hv	16.34%	1.49%	82.18%

(a) Summary

@Parking Lot		Recognition Result								
		no	ev5	ev10	ev20	ev30	hv5	hv10	hv20	hv30
Ground Truth	no	95.92%	0.09%	0.00%	0.09%	0.09%	0.53%	0.18%	0.89%	1.24%
	ev5	0.00%	97.06%	2.94%	0.00%	0.00%	0.00%	0.00%	0.00%	0.00%
	ev10	6.45%	6.45%	83.87%	3.23%	0.00%	0.00%	0.00%	0.00%	0.00%
	ev20	10.34%	0.00%	3.45%	86.21%	0.00%	0.00%	0.00%	0.00%	0.00%
	ev30	11.76%	0.00%	0.00%	5.88%	76.47%	0.00%	0.00%	0.00%	5.88%
Ground Truth	hv5	6.41%	0.00%	1.28%	1.28%	0.00%	70.51%	19.23%	1.28%	0.00%
	hv10	9.76%	0.00%	2.44%	0.00%	0.00%	31.71%	56.10%	0.00%	0.00%
	hv20	27.66%	0.00%	0.00%	0.00%	0.00%	0.00%	2.13%	57.45%	12.77%
	hv30	30.56%	0.00%	0.00%	0.00%	0.00%	2.78%	0.00%	16.67%	50.00%

(b) Details

Table 4. Confusion matrix of the detection performance of an EV and HV.

The figure also shows that the time the user receives the first alarm significantly changes depending on the vehicle speed. This is simply because the loudness of the EV noise is rather constant regardless of the vehicle speed. Thus, there is less time remaining before the vehicle approaches when the vehicle moves fast. At a speed faster than 30 km/h, road noise from tires becomes dominant, and there is no special need to detect only EVs. The figure also shows that the valiations in the environmental noise level affects the time that the vehicle can be detected. As previously mentioned, the ambient noise levels of the parking lot, residential area, and busy street were 37.6 dB, 40.6 dB and 58.7 dB respectively. As a general trend, earlier detection is possible in a quieter environment. Throughout this experiment, the earliest and latest alarms detected were at 11.6 s (in the residential area, 5 km/h) and 3.4 s (at the busy street, 30 km/h) before the vehicle approached the observer.

EV versus HV

The detection performance was measured when the data of the HV and EV were mixed. A comparison was performed using a dataset recorded in a parking lot. Table 4 is the confusion matrix as a result of 10-fold cross-validation. The false-positive rate is 4.08%, and the false-negative rate is 4.87%. The confusion matrix indicates that the EV and HV are clearly distinguished by the classifier. This is because the distribution in the bands in different, even though the switching noise from those two types of vehicles is found in similar frequency bands.

The result also shows that the true-positive value of the HV is lower than that of the EV. The reason appears to be that the HV is misclassified as no vehicle in a higher speed range (20 and 30 km/h). The spectrogram in Figure 5 also explains the results. The S-curve resulting from the switching noise is indistinct compared with that of the EV (Figure 4).

The cumulative percentage of the detection time is shown in Figure 9. From the figure, it is difficult to reach a clear conclusion that either the EV or HV is easier to detect earlier.

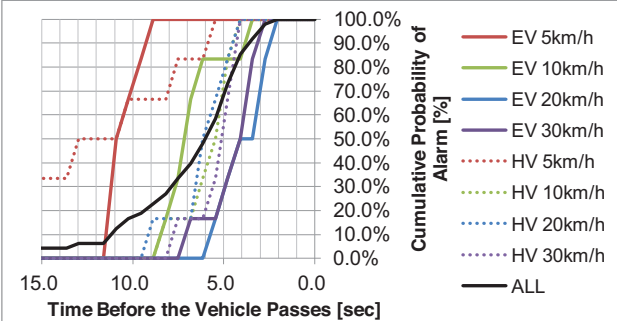


Figure 9. Comparison of an HV and EV in terms of the cumulative probability of the time alarms are fired.

This is mostly explained by the vehicle speed and the level of ambient noise.

DISCUSSION

Position of the Smartphone on the Body of a User

In the above measurements, we recorded the switching noise with a mobile handheld terminal. In this section, we recorded the switching noise in four positions simultaneously using four sets of lavalier microphones and iPod Touches in order to investigate the impact of the microphone position on the accuracy of EV detection. The four microphones were arranged on the temples of the glasses (assuming a microphone on a glass display device and/or a headphone), in the chest pocket, in the pants pocket and in a bag (Figure 10). We evaluated the cumulative probability of the detection alarm using the decision tree acquired in section , which is trained by the data recorded in the parking lot.

Figure 11 shows the cumulative probability for each of the four recording positions. At the position of the temple of the glasses, the detection accuracy of an approaching EV is comparable to the handheld case. When the microphone is placed in a pocket, the detection time is delayed for several seconds. The percentages of alarms lost when the microphone is in the chest pocket and pants pocket were approximately 20% and 36%, respectively. It should be noted that vehicle detection using a microphone in the pockets is possible although this is not the best detection condition. When the microphone was in a bag, no switching noise was detectable, and it was not possible to detect approaching vehicles.

Reducing the False-Negative Rate

This is a unique application where a false positive has insignificant cost to the pedestrian (maybe a look over the shoulder), but a false negative can be costly (an accident). Therefore, in this section, we discuss a method to reduce false-negatives at the expense of an increase in false positives.

In the experiment described in the previous sections, the segment in which the EV/HV was “visible” but not “audible” was not included in the training data to reduce ambiguity. In this section, we have included such segments so that these data are classified as “Vehicle is approaching.” According to Figure 12, the false-negative rate of the EV decreased from 6.3% to 0% and that of the HV decreased from 16.3% to



Figure 10. Position of the microphones during the measurement.

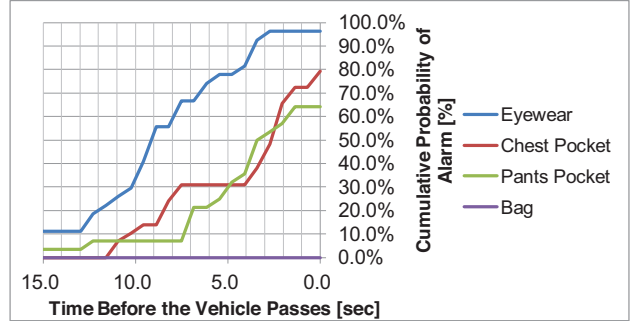


Figure 11. The cumulative probability for each of the four recording position.

@Parking Lot	Recognition Result			
	no	ev	hv	
Ground Truth	no	65.46%	13.07%	21.47%
	ev	0.00%	99.10%	0.90%
	hv	7.43%	3.96%	88.61%

Figure 12. Decision accuracy when the false-negative rate is reduced.

@Parking Lot		Recognition Result		
4096 sample / frame		no	ev	hv
Ground Truth	no	96.02%	0.73%	3.25%
	ev	15.57%	83.98%	0.44%
	hv	35.67%	0.38%	63.95%

(1) Frame Size = 4096 Samples (0.085 sec)				
@Parking Lot		Recognition Result		
8192 sample / frame		no	ev	hv
Ground Truth	no	96.70%	0.54%	2.76%
	ev	10.67%	88.89%	0.44%
	hv	29.02%	0.25%	70.73%

(2) Frame Size = 8192 Samples (0.171 sec)				
@Parking Lot		Recognition Result		
16384 sample / frame		no	ev	hv
Ground Truth	no	96.82%	0.29%	2.89%
	ev	7.62%	91.93%	0.45%
	hv	24.31%	0.00%	75.69%

(3) Frame Size = 16384 Samples (0.341 sec)				
@Parking Lot		Recognition Result		
32768 sample / frame		no	ev	hv
Ground Truth	no	95.92%	0.35%	3.73%
	ev	6.31%	92.79%	0.90%
	hv	16.34%	1.49%	82.18%

(4) Frame Size = 32768 Samples (0.682 sec)				
--	--	--	--	--

Figure 13. Relationship between the frame length and recognition accuracy.

7.4%. Simultaneously, the true-positive rate of “no EV/HV” state decreased from 95.9% to 65.5%. The authors believe that more user studies are needed to reach a clear conclusion on the balance between the false-positive rate and the false-negative rate. In addition to this adjustment, the consideration of state transitions is an alternative idea to reduce the number of false negatives while minimizing the number of false positives.

Power Consumption

Although we have not evaluated the power consumption of the smartphone, the best practice to extend the battery life of the smartphone is to divide the entire task into short tasks and to maximize the interval sleep time. Our detection scheme does not depend on the temporal correlation between frames, meaning that classification can be performed temporarily and independently. The length of the frame was only 0.683 s; thus, it was possible to incorporate sleep time without sacrificing detection accuracy. The FFT calculation of 32,768 samples was performed in real-time (< 0.683s) in addition to classification using the decision tree. It is probable that reducing the frame size contributes to extending the sleep time. However, the recognition results became worse as the frame size was shortened. This is because longer frames can smoothen the time variation of the spectrum and suppress the impact of undesired noise. Figure 13 shows the relationship between the frame length and the recognition accuracy.

IMPLEMENTATION ON ANDROID AND GOOGLE GLASS

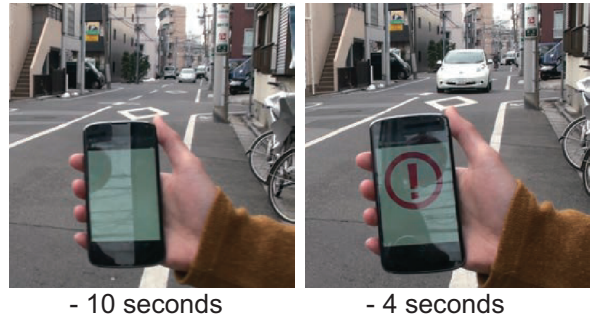


Figure 14. Implementation on a smartphone.

A smartphone is a powerful data processor that can detect EVs and HVs as we discussed. We have implemented the vehicle detection algorithm as an Android application and have performed a demonstration in a residential area. Figure 14 is a screenshot of the application running on a Nexus 4, an Android-based smartphone.

The classifier was trained in advance using the same training data used for the evaluation discussed in the previous section. The pictures on the left and right were captured 10 s and 4 s before the vehicle approached, respectively.

However, in general, using a smartphone while walking is not recommended. Thus, it is not the most suitable user interface device for notifying a user with a warning message. In this work, we propose using a wearable display to notify the user. In addition to the Android application mentioned above, we have implemented the notification system from an Android smartphone on Google Glass. When the Android application detects an approaching vehicle, a warning text and beeping sound appear on in the Google Glass of the user. When developing Google Glass applications (namely Glassware), developers have two API options. The Glass Development Kit (GDK) is the first option that allows developers access to low-level hardware features such as voice and gesture detection. Developers can use almost the same APIs as the standard Android SDK and can utilize the technical experience from Android development. This API is most suitable for implementing the vehicle detection algorithm on Google Glass for real-time user interaction. However, because of the limitations of the hardware of Google Glass, battery life and computational resources are quite limited. As a second choice, the Mirror API is provided. Using the Mirror API, developers simply need to develop a web-based service. The service runs in the cloud, and Google Glass automatically connects to the service over the Internet. For simplicity, we have implemented our notification system using an Android smartphone and Google Glass using the Mirror API.

As a drawback of the Mirror API, the smartphone and Google Glass cannot communicate with each other directly. Although the smartphone and Google Glass are placed next to each other (even if Google Glass is tethered to the smartphone), the notification message must be transferred to the server and delivered to Google Glass via Wi-Fi or a cellular network.

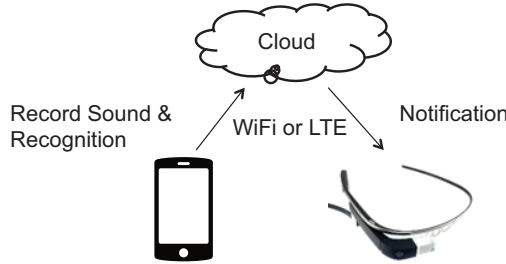


Figure 15. Implementation on Google Glass using the Mirror API.

This extra detour causes significant delay. We have measured this delay 20 times for each connection type including WiFi and LTE. The average delay through Wi-Fi and LTE were 3.41 s ($\sigma = 1.40$ s) and 3.39 s ($\sigma = 0.71$ s), respectively. According to Figure 8, in most cases except a busy street, the initial alarm was set off at least 5 s before the vehicle reached its closest distance. Although the system can alert users before the vehicle reaches its closest distance, this large time lag should be eliminated by implementing the vehicle detection algorithm on Google Glass using the GDK⁴.

RELATED WORKS

To the best of our knowledge, our proposal is the first to detect approaching EVs and HVs using high-frequency acoustic switching noise. The data can be processed on the mobile phone of the user and does not require infrastructure support.

In this section, several past approaches to detect vehicles on the road are introduced. Note that all of these methods are complementary. All of these past works can be integrated with our proposed method.

Pedestrian detection at a vehicle side is an important research area. Hundreds of studies have been reported in [5][1]. However, detecting approaching vehicles is a completely different endeavor.

Oki Electric Industry Co. Ltd. has developed a mobile phone that notifies the user of the presence of a vehicle using a DSRC[8]. This solution is not universally available because both the phone and car of the user must be equipped with DSRC, which has unfortunately not penetrated the market yet. Car-2-X[4] is a similar system that informs pedestrians about the presence of a car using ad-hoc and/or cellular networks.

An image-based approach is an alternative approach for the detection of moving vehicles. Sivaraman et al. proposed a general active-learning framework for on-road vehicle recognition and tracking based on video[10]. The Cyber-Physical Bike[11] is also an image-based vehicle detection scheme optimized for bicycles. In [14], Wang proposed an Android mobile phone application named WalkSafe. WalkSafe uses the back camera of a mobile phone to detect vehicles approaching the user. The benefit of the image based approach is that

⁴We are currently implementing the software using the GDK instead. Unfortunately, because of a lack of documentation, we could not report the results using the GDK. More details will be revealed when the camera ready version is complete.

it is possible to detect the trajectory of the vehicle, and this method can determine and assess the risk of collision in addition to detecting the approaching vehicles. The drawback of this approach is that the camera must be directed to the back of the user.

Tsuzuki has proposed a vehicle sound detection system for a mobile phone[12]. They classify the sound by using a standard LVQ neural network. The authors mention in the paper that all other existing solutions are too complex and not suitable for embedded devices. Unfortunately, the performance was only tested at speeds greater than 30 km/h and was focused on gasoline-engine vehicles. The proposed approach is not suitable for detecting silent EVs/HVs moving slower than 30 km/h. Even at 30 km/h, the car was detected 4.3 s before arrival according to [12]. In our experiment, the approach of the vehicle at 30 km/h was first detected 6.1 s before arrival in a residential area.

CONCLUSION

In this paper, we have demonstrated that high-frequency switching noise can be used to detect approaching HVs and EVs. Short pulses in the PWM switching used for IPM synchronous motors are the source of the noise. Because virtually all HVs and EVs are driven by IPM synchronous motors, this approach is effective for most commercial EVs and HVs.

We calculated the fingerprint of the target vehicles across multiple frequency bands near 5, 10, and 20 kHz. The experimental results revealed that this feature representation scheme is sufficiently robust to handle different environments while distinguishing the make, model, and speed of a vehicle. As for the detection of the approaching EVs in various environments, the false-positive rate was 1.2% and the false-negative rate was 4.95%. Note that our detection algorithm clearly distinguishes between the approaching and leaving vehicles. As a general trend, earlier detection is possible in a quieter environment. The earliest and latest alarms were detected 11.6 s (in the residential area, 5 km/h) and 3.4 s (on the busy street, 30 km/h) before the vehicle approached the observer.

Implementation of our system on an Android smartphone as well as Google Glass was introduced.

In contrast to existing vehicle detection methods based on infrastructure sensing schemes, image-based recognition schemes, and tire-noise detection schemes, our proposed method is most suitable for protecting pedestrians from being hit by careless drivers.

REFERENCES

1. Bu, F., and Chan, C. Y. Pedestrian detection in transit bus application: sensing technologies and safety solutions. In *Proceedings of IEEE Intelligent Vehicles Symposium* (June 2005), 100–105.
2. Cassat, A., Espanet, C., Coleman, R., Leleu, E., Burdet, L., Torregrossa, D., M'Boua, J., and Miraoui, A. Forces and vibrations analysis in industrial pm motors having concentric windings. In *IEEE Energy Conversion Congress and Exposition (ECCE)* (Sept 2010), 2755–2762.

3. Commision on measures for quietness of hybrid vehicles. Report on measures for quietness of hybrid vehicles. Goverment report of Ministry of Land, Infrastructure, Transport and Tourism, January 2010.
4. David, K., and Flach, A. Car-2-x and pedestrian safety. *IEEE Vehicular Technology Magazine* 5, 1 (March 2010), 70–76.
5. Gandhi, T., and Trivedi, M. Pedestrian protection systems: Issues, survey, and challenges. *IEEE Transactions on Intelligent Transportation Systems* 8, 3 (Sept 2007), 413–430.
6. New car sales ranking. <http://www.jada.or.jp/contents/data/ranking.html>, (in Japanese).
7. Incidence of pedestrian and bicyclist crashes by hybrid electric passenger vehicles, 2009. NHTSA Tech. Rep., DOT HS 811 204.
8. Oki Electric Industry Co., L. Oki succeeds in trial production of world's first "safety mobile phone" to improve pedestrian safety. Press release, May 2007.
9. Silent prius was exploited for robbery. the victim "didn't hear the car approaching". Asahi Shimbun, April 2010.
10. Sivaraman, S., and Trivedi, M. A general active-learning framework for on-road vehicle recognition and tracking.
11. IEEE Transactions on Intelligent Transportation Systems 11, 2 (June 2010), 267–276.
12. Smaldone, S., Tonde, C., Ananthanarayanan, V. K., Elgammal, A., and Iftode, L. The cyber-physical bike: A step towards safer green transportation. In *Proceedings of the 12th Workshop on Mobile Computing Systems and Applications*, HotMobile '11, ACM (New York, NY, USA, 2011), 56–61.
13. Tsuzuki, H., Kugler, M., Kuroyanagi, S., and Iwata, A. A novel approach for sound approaching detection. In *Neural Information Processing. Models and Applications*, K. Wong, B. Mendis, and A. Bouzerdoum, Eds., vol. 6444 of *Lecture Notes in Computer Science*. Springer Berlin Heidelberg, 2010, 407–414.
14. Wang, T., Cardone, G., Corradi, A., Torresani, L., and Campbell, A. T. Walksafe: A pedestrian safety app for mobile phone users who walk and talk while crossing roads. In *Proceedings of the Twelfth Workshop on Mobile Computing Systems and Applications*, HotMobile '12, ACM (New York, NY, USA, 2012), 5:1–5:6.